



Published in final edited form as:

*Radiat Res.* 2018 July ; 190(1): 45–52. doi:10.1667/RR14977.1.

## Acute effect of low-dose space radiation on mouse retina and retinal endothelial cells

X. W. Mao<sup>1</sup>, M. Boerma<sup>2</sup>, D. Rodriguez<sup>1</sup>, M. Campbell-Beachler<sup>1</sup>, T. Jones<sup>1</sup>, S. Stanbouly<sup>1</sup>, V. Sridharan<sup>2</sup>, A. Wroe<sup>3</sup>, G.A. Nelson<sup>1</sup>

<sup>1</sup>Department of Basic Sciences, Division of Radiation Research, Loma Linda University School of Medicine and Medical Center, Loma Linda, CA, U.S.A.

<sup>2</sup>Division of Radiation Health, Department of Pharmaceutical Sciences, University of Arkansas for Medical Sciences, Little Rock, AR, U.S.A.

<sup>3</sup>Department of Radiation Medicine, Loma Linda University School of Medicine and Medical Center, Loma Linda, CA, U.S.A.

### Abstract

There is concern that degradation of vision as a result of space flight may compromise both mission goals and long-term quality of life after space travel. The visual disturbances may be due to a combination of intracerebral pressure changes and exposure to ionizing radiation. The retina and the retinal vasculature play important roles in vision, yet have not been studied extensively in relation to space travel and space radiation. The goal of the present study was to characterize oxidative damage and apoptosis in retinal endothelial cells after whole-body gamma-ray, proton and oxygen (<sup>16</sup>O) ion radiation exposure at 0.1 to 1 Gy. Six month old male C57Bl/6J mice were exposed whole-body to 600 MeV/n <sup>16</sup>O ions (0, 0.1, 0.25, 1 Gy), solar particle events (SPE)-like protons (0, 0.1, 0.25, 0.5 Gy) or <sup>60</sup>Co gamma-rays (0, 0.1, 0.25, 0.5 Gy). Eyes were isolated for examining endothelial nitric oxide synthase (eNOS) expression and characterization of apoptosis in retina and retinal endothelial cells at 2 weeks post irradiation. The expression of eNOS was significantly increased in the retina following proton and <sup>16</sup>O ions exposure. <sup>16</sup>O ions induced over 2-fold increase in eNOS expression compared to protons at the 2-week post irradiation time point (p<0.05). TUNEL assays showed dose dependent increases in apoptosis in the retina following irradiation. Low doses of <sup>16</sup>O ions elicited apoptosis in the mouse retinal endothelial cells with the most robust changes observed after 0.1 Gy exposure (p<0.05) compared to controls. Data also showed that <sup>16</sup>O ions induced a higher frequency of apoptosis in retinal endothelial cells as compared to protons (p<0.05). In summary, our study revealed that exposure to low-dose ionizing radiation induced oxidative damage and apoptosis in the retina. Significant changes in retinal endothelial cells occur at doses as low as 0.1 Gy. There were significant differences in the responses of endothelial cells between radiation types.

### INTRODUCTION

There is concern that degradation of vision as a result of space flight may compromise both mission goals and long-term quality of life after space travel (1). These visual disturbances associated with space travel may be due to a combination of altered gravitation changes (2) and exposure to ionizing radiation (3). A unique feature of the space radiation environment

is the presence of high-charge high-energy particles (HZE) of the galactic cosmic ray (GCR) environment and proton-rich solar particle events (SPE). These GCR ions and protons present a significant hazard to space-flight crews in the course of their activities. The eye is a unique organ because it is relatively unprotected and is constantly exposed to radiation, atmospheric oxygen, environmental chemicals, and physical abrasion. Nonetheless, the retina and the retinal vasculature have not been studied extensively in relation to space travel and space radiation especially increased radiation risks beyond the low earth orbit (LEO).

The adverse effects of radiation on the retina (4–6) and retinal vasculature (7–8) have been reported by multiple investigators who have documented histopathological and functional alterations in the affected retina and retinal microvasculature post-irradiation. Our previous analysis of the microvasculature in the rat retina showed a time- and dose-dependent, progressive loss of endothelial cells and microvessel length over a period of two years following proton radiation (9). However, most of the animal and clinical data with patients and occupational studies from which the current knowledge of radiation-induced retinal injury is obtained, is based on relatively high doses of photon radiation. Little is known about the susceptibility to low doses of ionizing radiation, and charged particle radiation, in particular.

Radiation-induced cell damage involves generation of reactive oxygen species (ROS) in the cell (10). Free radical-induced ocular tissue damage has been associated with a variety of pathological conditions, such as cataracts (11), age-related macular degeneration (12), and experimental autoimmune uveitis (13). Oxidative stress is likely to be involved in the pathogenesis of radiation-induced retinal damage (14). The retina contains a high level of polyunsaturated fatty acids, making it more susceptible to lipid peroxidation (15). We have shown that space travel and space-like radiation exposures cause oxidative changes in the retina and continuous remodeling of retinal microvessel architecture over the course of a year after irradiation (9, 16, 17). Many studies have shown that oxidative stress constitutes a biochemical mechanism regulating cell function and the ultimate fate of cells (18). Studies also have shown that radiation at doses less than 1 Gy induced significant levels of oxidative stress in the brain (19) and neural precursor cells (20). Accumulating evidence suggests ROS interfere with nitric oxide (NO) regulation produced by endothelial NO synthase (eNOS) causing endothelial dysfunction (21). Increased production of superoxide may also react with NO to form peroxynitrite (ONOO<sup>-</sup>), thus inducing nitrosative stress. Overproduction of ROS and nitrogen (RNS) species results in destruction of cellular structures and induce apoptotic cell death (22).

The goal of the present study was to investigate the effects of whole-body <sup>16</sup>O exposure on apoptosis and oxidative stress in retinal endothelial cells and to compare these radiation-induced effects with those produced by SPE-like proton or gamma-ray exposure.

## MATERIAL AND METHODS

### Animals and radiation with oxygen ions

One to 2-month-old male C57BL/6J mice were purchased from the Jackson Laboratory (Bar Harbor, ME) and delivered to the University of Arkansas for Medical Sciences (UAMS)

where they were housed in standard caging on a 12-hour day/night cycle and received standard rodent chow low in soy (2020X, Harlan Laboratories) and water ad libitum. At 6 months of age, mice were shipped to Brookhaven National Laboratories (BNL) in Upton, NY. After a one-week acclimation period, the mice were either sham irradiated or received whole-body  $^{16}\text{O}$  irradiation (600 MeV/n; 0.1, 0.25 and 1.0 Gy, dose rate: 0.25 – 0.26 Gy/min, n=10/group). Dosimetry was performed by the NASA Space Radiation Laboratory physics dosimetry group at BNL to ensure the quality of exposure. For each exposure, unanesthetized animals were individually placed into clear Lucite boxes (3 in x 1½ in x 1½ in) with breathing holes. Sham irradiated mice were placed into the same enclosures for the same amount of time, but were not exposed to radiation. One day after irradiation, the mice were returned to UAMS, where they were housed under conditions described above. All procedures were approved by the Institutional Animal Care and Use Committee at UAMS and BNL.

### **Animals and irradiation with SPE-like proton and gamma-ray**

6-month-old C57BL/6 male mice, each weighing between 30–35 grams, were purchased from the Jackson Laboratory (Bar Harbor, ME) and shipped to Loma Linda University in Loma Linda CA. Animals were maintained under a constant temperature of 68°F with a 12-hour day/night cycle. Chow and water were available ad libitum. After a one-week acclimation period, the mice were either sham irradiated or received whole-body SPE-like proton irradiation at 0.1, 0.25 and 0.5 Gy (n = 8/group). The mice were restrained individually in 1-mm thick, rectangular plastic boxes (3 × 3 × 8.5 cm) with air holes. The proton beam was orientated at zero degrees such that the mice were dorsally irradiated. SPE-like exposures were simulated by using a fully modulated 149.6 MeV/n proton beam. The full modulation of the monoenergetic proton beam was produced by passing it through a rotating propeller-like modulator wheel with 21 thickness steps machined into the blades to range shift the single incident proton energy into 21 separate proton energies. Utilizing a 2.1 cm thick water equivalent range shifter, the lowest Bragg peak energy was 39 MeV, while the highest was 122 MeV. The superposition of 21 Bragg peaks created a uniform dose region (known as the spread-out Bragg peak) across the entire animal regardless of its orientation within the holder. Unirradiated controls were immobilized for the same length of time, positioned in the proton irradiation field without exposure (sham irradiation).

For comparison, whole-body  $^{60}\text{Co}$  irradiations were completed to estimate the relative biological effectiveness (RBE) responses. For  $^{60}\text{Co}$  irradiations, mice were restrained individually in 1-mm thick, rectangular plastic boxes (3 × 3 × 8.5 cm) with air holes.  $^{60}\text{Co}$  dose was delivered using an AEC Eldorado therapy unit (Atomic Energy Canada, Commercial Products Division, Ottawa, Canada). The  $^{60}\text{Co}$  radiation beam was orientated at zero degrees such that the mice were dorsally irradiated and a 0.5 cm water equivalent range shifter was used to place  $D_{\text{max}}$  inside the animal. Animals were irradiated with a single exposure from a  $^{60}\text{Co}$  source to a total dose of 0.1, 0.25 and 0.5 Gy. The average dose rate for irradiations was 0.827 ± 0.001 Gy/min and the dose uniformity of irradiations was +/– 2%. Dose delivery was redundantly calibrated using both an Exradin A12 and T1 ionization chamber, coupled with a Standard Imaging MAX4000 electrometer. Both ionization chambers were calibrated by an Accredited Dosimetry Calibration Laboratory

(ADCL) traceable to the National Institute of Standards and Technology. Unirradiated animal controls were immobilized for the same length of time, and positioned on the Cobalt irradiator without delivering radiation (sham irradiation).

### Eye and retina preparation

At 2 weeks after proton and gamma-ray exposure, and at 2 weeks after  $^{16}\text{O}$ , mice were euthanized and the right eye from each mouse was placed individually in sterile cryovials, snap frozen in liquid nitrogen and kept at  $-80^{\circ}\text{C}$  prior to use. The left eyes were fixed in 4% paraformaldehyde in phosphate buffered saline (PBS) for immunohistochemistry (IHC) assays.

### Immunohistochemistry assays and histology

To characterize apoptosis, sections of the eyes were subjected to a terminal deoxynucleotidyltransferase dUTP nick-end labeling (TUNEL) staining. 6  $\mu\text{m}$  paraffin-embedded sections roughly 100  $\mu\text{m}$  apart were deparaffinized in Histo-Clear, then permeabilized in proteinase K solution. Retinal tissues were evaluated using the DeadEnd™ Fluorometric TUNEL system kit (catalog no. G3250, Promega Corp., Madison, WI). The same sections were then incubated with DyLight 594 Lycopersicon Esculentum-Lectin (catalog no: DL-11721, Vector Laboratories,) at a 1:100 dilution for 30 minutes at room temperature to stain the endothelium. Nuclei were counterstained with diamidino-2-phenylindole (DAPI, blue). Sections were examined using a BZ-X710 All-in-One inverted fluorescence microscope with structural illumination (Keyence Corp., Elmwood Park, NJ). TUNEL-positive cells were identified by green fluorescence, vascular endothelial cells were identified with red fluorescence.

To characterize eNOS expression in retina and retinal endothelial cells, the ocular sections were incubated with rabbit anti-Endothelial Nitric Oxide Synthase (eNOS) primary antibody (catalog no. ab5589, Abcam) at a 1:100 dilution at  $37^{\circ}\text{C}$  for 1 hour, followed by a goat anti-rabbit IgG DyLight 594 secondary antibody (catalog no: 35561, Thermo Scientific) at a 1:200 dilution for 1 hour at room temperature. Sections were then stained with DyLight 488 Lycopersicon Esculentum-Lectin (catalog no: DL-11721, Vector Laboratories,) at a 1:100 dilution for 30 minutes at room temperature. eNOS immunoreactivity was identified by red fluorescence; vascular endothelial cells were identified with green fluorescence, the nuclei of retinal cells were counterstained with DAPI (blue fluorescence).

For quantitative analysis, the total number of TUNEL or eNOS-positive cells in the retina, and the number of TUNEL or eNOS positive cells in the retinal vessels (double staining with lectin) were determined in ten sections of each eye. The area of the retina was measured on digital microphotographs using ImageJ counting plugin 1.41 software (National Institutes of Health, Bethesda, MD; <http://rsbweb.nih.gov/ij/>), and the density profiles were expressed as mean number of apoptotic or eNOS positive cells/ $\text{mm}^2$ . Similar procedures for density evaluation have been described in our previous paper (16). The mean of the density profile measurements across ten retina sections per eye was used as a single experimental value.

## Statistical Analysis

The results obtained from all experiments were analyzed by one-way analysis of variance (ANOVA) followed by Tukey's post hoc multiple-comparison test (SigmaPlot for Windows, version 13.0; Systat Software, Inc., Point Richmond, CA). The significance level was set at  $p < 0.05$ . Data are shown as mean  $\pm$  standard error (SEM).

## RESULTS

### Apoptosis in retinal endothelial cells following $^{16}\text{O}$ or proton irradiation

TUNEL assays showed that  $^{16}\text{O}$  irradiation induced significant apoptosis at 2 weeks following irradiation at doses of 0.1 to 1 Gy. The most prominent TUNEL positive staining was seen in the inner nuclear layer (INL) and inner plexiform layer (Figure 1). Our quantitative assessment revealed that TUNEL positive retinal endothelial cell density was significantly higher following irradiation at 0.1, 0.25 and 1 Gy compared to controls ( $p < 0.05$ ) (Figure 2). The most robust changes were observed after 0.1 Gy (30.1 apoptotic cells/mm<sup>2</sup>) compared to control (9.2 apoptotic cells/mm<sup>2</sup>).

At 2 weeks following proton irradiation, the increase of apoptosis in retinal endothelial cells was most pronounced in retinas that received 0.5 Gy (18.2/mm<sup>2</sup>) as compared to the controls (10.5/mm<sup>2</sup>) ( $p < 0.05$ ). However, apoptotic retinal endothelial cell counts were significantly lower (about 2-fold) following proton irradiation compared to  $^{16}\text{O}$  irradiation at doses of 0.1 and 0.25 Gy, suggesting that oxygen is more effective in inducing apoptosis than protons (Figure 2).

### Comparison of radiation effect on retinal apoptosis following $^{16}\text{O}$ or proton irradiation

TUNEL positive non-endothelial cells were also quantified. At 2 weeks post proton irradiation, a radiation-induced increase in non-endothelial cell apoptosis in the retina was detected and ranged from a 1.7 to 1.9-fold increase for protons compared to controls. Doses of 0.1, 0.25 and 0.5 Gy of protons resulted in a significant increase of apoptotic cell death in the retina ( $p < 0.05$ ) (Figure 3).  $^{16}\text{O}$  exposure also significantly increased apoptosis in the retina at 2-weeks following 0.1 to 1 Gy exposure ( $p < 0.05$ ). The increase ranges from 1.3 to 1.5-fold compared to controls.

### eNOS immunoreactivity following $^{16}\text{O}$ or proton irradiation

Increased eNOS staining was seen in the retinal INL, inner plexiform layer and ganglion cell layer (GCL) following 0.1–1 Gy (Figure 4) of  $^{16}\text{O}$  radiation. Our analysis indicated that increased expression of eNOS immunoreactivity in retinal endothelial cells was more pronounced following oxygen irradiation compared to the proton radiation (Figure 5). For non-endothelial cells, there were significant increases of eNOS immunoreactivity in the retina after 0.1–1 Gy of  $^{16}\text{O}$  irradiation compared to 0 Gy ( $p < 0.05$ ). Following proton radiation, eNOS immunoreactivity in non-endothelium retinal cells was significantly higher at 0.5 Gy compared to control and the 0.25 Gy group (Figure 6).

## Relative biological effectiveness (RBE) estimate for total apoptosis in the retina at two weeks following irradiation

For total apoptosis in the retina, the  $RBE_M$  (ratio of tangents of dose responses at 0 dose) was estimated by fitting data to 2<sup>nd</sup> order polynomials and determining the slopes of the first derivative at  $D = 0$  (23). These fits gave greater  $R^2$  values than linear equation fits. Table 1 lists the equations,  $R^2$  values, and ratios of slopes (slope H or O / slope  $\gamma$ ) at  $D = 0$ . Thus  $RBE_{MS}$  for protons and oxygen are estimated at 1.60 and 2.28 respectively.

## DISCUSSION

Space radiation is dominated by charged particles. These include a variety of high-energy (E) and high-charge (Z) ions (i.e. HZE particles; >100 MeV/nucleon) with high-linear energy transfer (LET). Potential exposures to charged particles are a significant radiation hazard to astronauts and spacecraft electronics and present a major challenge for the National Aeronautics and Space Administration (NASA). During long-term deep space missions, it is anticipated that exposure to GCR and SPEs may place astronauts at risk for acute radiation sickness (ARS), prodromal effects, skin damage, hematological/immune deficits, and changes in other body compartments. The timing of symptom onset varies with radiation dose, dose rate, quality and individual sensitivity (24–26).

Galactic cosmic rays are fully ionized atomic nuclei, and other subatomic particles produced by energetic sources outside of the solar system such as stars and highly energetic objects such as supernovae. The abundance of GCR by Z reflects the cosmic abundance of elements. By far the most abundant component is hydrogen nuclei or protons (numerically about 85% of the fluence) followed by helium nuclei (about 13%) followed by other elements up to iron ( $Z = 26$ ) with even number elements such as  $^{12}\text{C}$ ,  $^{16}\text{O}$ , and  $^{28}\text{Si}$  being more abundant than odd numbered elements (27). Due to the unique properties of the HZE particles, their biological impact is qualitatively different compared to conventional sparsely ionizing photon radiation: 1) Traversals of HZE particles may physically damage biomolecules; 2) Dense ionization in the core of tracks of the primary particles and the generation of secondary  $\delta$ -rays results in clustered damage to molecular and subcellular structures that are poorly repairable by cell protective mechanisms (28); 3) High LET radiation promotes the formation of ROS (29,30) and lipid peroxidation (31,32).

A limited number of studies were performed to evaluate the impact of low-dose charge particles and simulated SPE in biological systems, especially in the central nervous system (CNS). The objective of the present study was to determine the effects of radiation dose and quality on retina and retinal endothelial cells. We characterized acute and early low-dose radiation induced retinal endothelial cell damage as measured by apoptosis. To our knowledge, this is the first study to examine the impact of low-dose oxygen ions and simulated SPE on neurovascular damage and compare biological effects of these two species of charged particles.

As a measure of track intensity, LET has been used (33). LET is the energy transferred to the target per unit length of track. The high LET character of heavy ions such as  $^{16}\text{O}$  ions is expected to result in higher RBEs compared to low-LET protons or photons (34). Relative

biological effectiveness can be considered as a useful parameter for comparison when investigating the outcome in terms of experimental models established on biologically related parameters (35). Our study revealed that  $^{16}\text{O}$  was most effective in inducing apoptosis followed by proton and  $^{60}\text{Co}$  gamma-rays, in that order. An estimated RBE for total retinal cell apoptosis was around 2.3 for oxygen and 1.6 for protons at the 2-week time point. Our results are consistent with the association of higher RBE-values with relatively higher charge and LET particles.

A healthy vasculature is needed for proper functioning of all tissues but is vulnerable to environmental insults, including space travel and ionizing radiation. The ability of blood vessels to sense and respond to stimuli, such as fluid flow, shear stress, and trafficking of immune cells is critical to the proper functioning of the vasculature (36). Previous studies have shown that vascular endothelial cells are a critical target population responsible for radiation-induced CNS injury (37,38). One observation from the present investigation showed that endothelial cell apoptosis accounts for over 50% of total cell apoptosis in the retina for both  $^{16}\text{O}$  and proton exposure. Our finding is in agreement with others that the vasculature is vulnerable following radiation insults and constitutes a critical dose-limiting tissue component of the CNS (39,40). The retina has a high demand for oxygen to maintain its function (41). Loss of vascular endothelium could result in damage of photoreceptor structure and function.

eNOS is an important cell signaling molecule that catalyzes the production of nitric oxide (NO) in the vascular wall. One of the hallmarks of endothelial dysfunction is oxidative stress, which is a critical contributor to the pathophysiological manifestations of vascular injury (42). Our previous studies have shown that spaceflight and ionizing radiation induce prolonged endothelial dysfunction, thereby sustaining a detrimental tissue environment associated with chronic inflammation and maladaptive tissue remodeling (17). Nitric oxide is synthesized by eNOS as well as neural NOS (nNOS) and inducible NOS (iNOS). Endothelial production of NO is critical to the regulation of vascular responses, including vascular tone and regional blood flow, and leukocyte–endothelial interaction (43). Alteration of eNOS activity can be major sources of ROS in endothelial dysfunction (44). Studies have shown that the activity of eNOS was significantly increased in irradiated cells (45). Ionizing radiation is associated with increased oxidative stress markers and eNOS activation in endothelial cells (46). eNOS also plays a role in regulation of apoptosis after irradiation (47). Our current data do suggest that ionizing radiation, especially heavy ion charge particles may activate eNOS, promote apoptosis in retinal endothelial cells, and contribute to endothelial dysfunction.

The greater response observed for the retinal endothelial cells following 0.1 Gy of  $^{16}\text{O}$  compared to higher doses of 0.25 and 1 Gy was very interesting. This complex dose-effect relationship was also observed in our previous study (16), and nonlinear ionizing radiation-induced changes were also seen in the lens epithelium (48). The mechanism for this type of nonlinear biological response remains to be determined. It is possible that apoptotic processes and their timing following lower doses of ionizing radiation is different compared to higher doses. Another possibility is that low dose radiation-induced damage is not sufficient to activate DNA damage detection and repair. However, at higher doses of

radiation exposure, intracellular overproduction of ROS and nitrogen (RNS) facilitated by eNOS activation elicits DNA repair function and antioxidant defense.

In summary, our data revealed that exposure to low doses of ionizing radiation induced apoptosis in the retina. Significant changes in retinal endothelial cells occur at doses as low as 0.1 Gy. There was significant differences in the response of endothelial cells between radiation types. We proposed that radiation-induced changes might be associated with eNOS activation. Diverse changes in response to different radiation quality and dose warrants further investigation. Further studies are also necessary to elucidate possible mechanism for coordinative regulation of endothelial cell apoptosis by eNOS responsible for our findings.

## ACKNOWLEDGEMENTS

This study was supported by National Space Biomedical Research Institute (NSBRI) grant #RE03701 through NASA cooperative agreement NCC 9-5884. The authors would also like to thank Dr. Jerry D. Slater and James M. Slater Proton Therapy Treatment & Research Center, LLUMC for the support.

## REFERENCES

1. Mader TH, Gibson CR, Pass AF, Kramer LA, Lee AG, Fogarty J, et al. Optic disc edema, globe flattening, choroidal folds, and hyperopic shifts observed in astronauts after long-duration space flight. *Ophthalmology*. 2011; 118(10):2058–69. [PubMed: 21849212]
2. Nelson ES, Mulugeta L, Myers JG. Microgravity-induced fluid shift and ophthalmic changes. *Life (Basel)*. 2014; 4: 621–665. [PubMed: 25387162]
3. Philpott DE, Corbett R, Turnbull C, Harrison G, Leaffer D, Black S, Sapp W, Klein G, Savik LF. Cosmic ray effects on the eyes of rats flown on Cosmos No. 782, experimental K-00.7. *Aviat Space Environ Med* 1978; 49: 19–28. [PubMed: 623561]
4. Mayer M, Kaiser N, Layer PG, Frohns F. Cell Cycle Regulation and Apoptotic Responses of the Embryonic Chick Retina by Ionizing Radiation. *PLoS One*. 2016;11(5):e0155093.
5. Frizziero L, Parrozzani R, Midena G, Miglionico G, Vujosevic S, Pilotto E, Midena E. Hyperreflective intraretinal spots in radiation macular edema on spectral domain optical coherence tomography. *Retina*. 2016; 36(9):1664–9. [PubMed: 26960014]
6. Vinogradova IuV Tronov VA, Liakhova KN Poplinskaia VA, Ostrovskii MA. Damage and functional recovery of the mouse retina after exposure to ionizing radiation and methylnitrosourea. *Radiats Biol Radioecol*. 2014; 54(4):385–92. [PubMed: 25775827]
7. Toutounchian JJ, Steinle JJ, Makena PS, Waters CM, Wilson MW, Haik BG, Miller DD, Yates CR. Modulation of radiation injury response in retinal endothelial cells by quinic acid derivative KZ-41 involves p38 MAPK. *PLoS One*. 2014; 9(6):e100210.
8. Fedirko PA, Babenko TF, Dorichevska RY, Garkava NA. Probl Radiac Med Radiobiol. Retinal vascular pathology risk development in the irradiated at different ages as a result of chernobyl NPP accident. *Probl Radiac Med Radiobiol* 2015; 20:467–573. [PubMed: 26695923]
9. Mao XW, Archambeau JO, Kubinova L, Boyle S, Petersen G, Grove R: Quantification of rat retinal growth and vascular population changes after single and split doses of proton irradiation: translational study using stereology methods. *Radiat Res* 2003; 160(1):5. [PubMed: 12816518]
10. von Sonntag C, *The Chemical basis of radiation biology* Taylor and Francis, London 1987.
11. Shichi H Cataract formation and prevention. *Expert Opin Investig Drugs* 2004; 13(6):691–701.
12. Beatty S, Koh H, Phil M, Henson D, Boulton M. The role of oxidative stress in the pathogenesis of age-related macular degeneration. *Surv Ophthalmol* 2000; 45(2):115–34. [PubMed: 11033038]
13. Wu GS, Zhang J, Rao NA. Peroxynitrite and oxidative damage in experimental autoimmune uveitis. *Invest Ophthalmol Vis Sci* 1997; 38(7):1333–9. [PubMed: 9191596]
14. van Reyk DM, Gillies MC, Davies MJ. The retina: oxidative stress and diabetes. *Redox Rep* 2003; 8(4):187–92. [PubMed: 14599341]



15. Ohia SE, Opere CA, Leday AM. Pharmacological consequences of oxidative stress in ocular tissues. *Mutat Res* 2005; 11: 579(1–2):22–36. [PubMed: 16055157]
16. Mao XW, Pecaut MJ, Stodieck LS, Ferguson VL, Bateman TA, Bouxsein M, Jones TA, Moldovan M, Cunningham CE, Chieu J and Gridley DS. Space Flight Environment Induces Mitochondrial Oxidative Damage in Ocular Tissue. *Radiat Res* 2013; 180:340–50. [PubMed: 24033191]
17. Mao XW, Favre C, Fike JR, Kubinova L, Anderson E, Campbell-Beachler M, Jones T, Smith A, Rightnar S and Nelson GA. High-LET radiation-induced response of microvessels in the hippocampus. *Radiat Res* 2010; 173:486–93. [PubMed: 20334521]
18. Noble M, Smith J, Power J, Mayer-Proschel M. Redox state as a central modulator of precursor cell function. *Ann N Y Acad Sci* 2003; 991:251–271. [PubMed: 12846992]
19. Burlaka AP, Druzhyna MO, Vovk AV, Lukin SM. Disordered redox metabolism of brain cells in rats exposed to low doses of ionizing radiation or UHF electromagnetic radiation. *Exp Oncol* 2016; 38(4):238–241. [PubMed: 28230822]
20. Limoli CL, Giedzinski E, Baure J, Rola R, Fike JR. Redox changes induced in hippocampal precursor cells by heavy ion irradiation. *Radiat Environ Biophys* 2007; 46:167–172. [PubMed: 17103219]
21. Pennahur S, Heinecke JW. Oxidative stress and endothelial dysfunction in vascular disease. *Curr Diab Rep* 2007;7(4):257–64. [PubMed: 17686400]
22. Olgúin Albuerne M, Ramos-Pittol JM, Coyoy A, Martínez-Briseño CP, Domínguez G, Morán J. Peroxynitrite is Involved in the Apoptotic Death of Cultured Cerebellar Granule Neurons Induced by Staurosporine, but not by Potassium Deprivation *Neurochem Res*. 2016; 41(1–2):316–27. [PubMed: 26700430]
23. Wu H, Huff JL, Casey R, Kim MH, Cucinotta FA. Evidence Report: Risk of Acute Radiation Syndromes Due to Solar Particle Events. Houston, TX: National Aeronautical and Space Agency 2013.
24. ICRP Relative Biological Effectiveness (RBE), Quality Factor (Q), and Radiation Weighting Factor (wR). Recommendations of the International Commission on Radiological Protection. ICRP Publication 92, 2003.
25. Chanellor JC, Scott GB, Sutton JP. Space Radiation: The Number One Risk to Astronaut Health beyond Low Earth Orbit. *Life (Basel)* 2014; 4(3), 491–510. [PubMed: 25370382]
26. Kennedy AR. Biological Effects of Space Radiation and Development of Effective Countermeasures. *Life Sci Space Res (Amst)*, 2014; 1: 10–43. [PubMed: 25258703]
27. Mewltd R Elemental Composition and Energy Spectra of Galactic Cosmic Rays In: Feynman J, Gabriel S, editors. Interplanetary Particle Environment: Proceedings of a Conference; 1988; JPL Publication 88–28.
28. Broos AL, Bao S, Rithidech K, Chrisler WB, Couch LA and Braby LA. Induction and repair of HZE induced cytogenetic damage. *Phys Med* 17 Suppl 2001; 1:183–4.
29. Mozmdar A Early production of radicals from charged particle tracks in water. *Radiat Res Suppl* 1985; 8:S33–39. [PubMed: 3867087]
30. Giedzinski E, Rola R, Fike JR and Limoli CL. Efficient production of reactive oxygen species in neural precursor cells after exposure to 250 MeV protons. *Radiat Res* 2005; 164: 540–4. [PubMed: 16187784]
31. Karbownik M and Reiter RJ, Antioxidative effects of melatonin in protection against cellular damage caused by ionizing radiation. *Proc Soc Exp Biol Med*, 2000; 225(1): 9–22. [PubMed: 10998194]
32. de Zwart LL, Meerman JH, Commandeur JN, and Vermeulen NP, Biomarkers of free radical damage applications in experimental animals and in humans. *Free Radic Biol Med*. 1999; 26(1–2): 202–26. [PubMed: 9890655]
33. Kraft G Blakely EA, Hieber L, Kraft-Weyrather W, Miltenburger HG, Muller W, Schuber M, Tobias CA, Wulf H. HZE effects on mammalian cells. *Adv Space Res*. 1984; 4(10):219–26. [PubMed: 11539630]
34. Bassler N, Toftegaard J, Luhr A, Sorensen BS, Scifoni E, et al. LET-painting increases tumour control probability in hypoxic tumours. *Acta Oncol* 2014; 53:25–32. [PubMed: 24020629]

35. Baiocco G, Alloni D, Babini G, Mariotti L and Ottolenghi A. Reaction mechanism interplay in determining the biological effectiveness of neutrons as a function of energy Radiat. Prot. Dosim. 2015; 166 316–319.
36. Wilson CW, Ye W. Regulation of vascular endothelial junction stability and remodeling through Rap 1- Rasip1 signaling. Cell Adh Migr 2014; 8:76–83. [PubMed: 24622510]
37. Lyubimova N and Hopewell JW, Experimental evidence to support the hypothesis that damage to vascular endothelium plays the primary role in the development of late radiation induced CNS injury. Br. J. Radiol. 2004; 77, 488–492. [PubMed: 15151969]
38. Morris GM, Coderre JA, Bywaters A, Whitehouse E, Hopewell JW. Boron neutron capture irradiation of the rat spinal cord: histopathological evidence of a vascular-mediated pathogenesis. Radiat Res 1996; 146(3):313–20. [PubMed: 8752310]
39. Amoaku WMK, Archer DB. Cephalic radiation and retinal vasculopathy. Eye 1990; 4:195–203. [PubMed: 2323471]
40. Merriam GR, Focht EF. The effects of ionizing radiation on the eye. Front Rad Ther Oncol 1972; 6:346–385.
41. Yu DY, Cringle SJ. Oxygen distribution and consumption within retina in vascularized and avascular retinas and in animal models of retinal disease. Prog Retin Eye Res. 2001; 20:175–208. [PubMed: 11173251]
42. Kowluru RA. Diabetic retinopathy: mitochondrial dysfunction and retinal capillary cell death. Antioxid Redox Signal 2005; 7: 1581–7. [PubMed: 16356121]
43. Atochin DN, Huang PL. Endothelial nitric oxide synthase transgenic models of endothelial dysfunction. Pflugers Arch. 2010; 460(6):965–74. [PubMed: 20697735]
44. Rouaud F, Romero-Perez M, Wang H, Lobysheva I, Ramassamy B, Henry E, Tauc P, Giaccherio D, Boucher JL, Deprez E, Rocchi S, Slama-Schwok A. Regulation of NADPH-dependent Nitric Oxide and reactive oxygen species signalling in endothelial and melanoma cells by a photoactive NADPH analogue. Oncotarget. 2014; 5(21):10650–64. [PubMed: 25296975]
45. Nagane M, Yasui H, Sakai Y, Yamamori T, Niwa K, Hattori Y, Kondo T, Inanami O. Activation of eNOS in endothelial cells exposed to ionizing radiation involves components of the DNA damage response pathway. Biochem Biophys Res Commun. 2015; 456(1):541–6. [PubMed: 25498542]
46. Sakata K, Kondo T, Mizuno N, Shoji M, Yasui H, Yamamori T, Inanami O, Yokoo H, Yoshimura N, Hattori Y. Roles of ROS and PKC- $\beta$ II in ionizing radiation-induced eNOS activation in human vascular endothelial cells. Vascul Pharmacol. 2015; 70:55–65. [PubMed: 25869503]
47. Weller R, Billiar T, Vodovotz Y. Pro- and anti-apoptotic effects of nitric oxide in irradiated keratinocytes: the role of superoxide. Skin Pharmacol Appl Skin Physiol. 2002; 15:348–352. [PubMed: 12239430]
48. Markiewicz E, Barnard S, Haines J, Coster M, van Geel O, Wu W, Richards S, Ainsbury E, Rothkamm K, Bouffler S, Quinlan RA. Nonlinear ionizing radiation-induced changes in eye lens cell proliferation, cyclin D1 expression and lens shape. Open Biol. 2015; 5(4):150011.

## TUNEL, Endothelium, DAPI

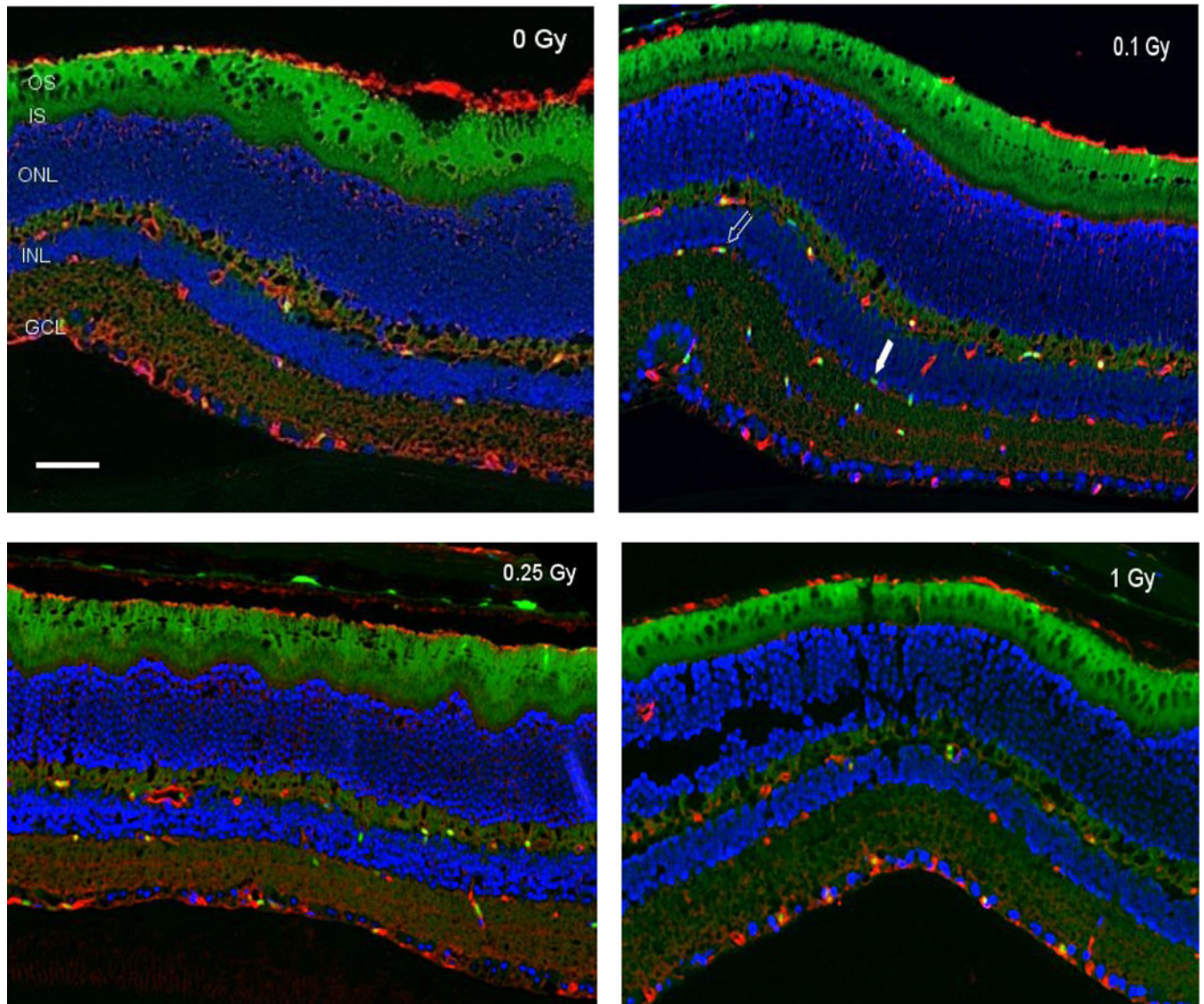


**Figure 1:** Apoptosis based on terminal deoxynucleotidyltransferase dUTP nick-end labeling (TUNEL) staining of retinal tissue. Representative micrographs of sections that were evaluated at 2 weeks after  $^{16}\text{O}$  radiation. a) control, b) 0.1 Gy, c) 0.25 Gy and d) 1 Gy. TUNEL-positive cells were identified with green fluorescence, endothelium was stained with lectin (red). The nuclei of photoreceptors were counterstained with DAPI (blue). In the control retinal tissue, only sparse TUNEL-positive cells were found. In the retina from mice exposed to 0.1 Gy of  $^{16}\text{O}$  radiation, TUNEL-positive labeling was apparent in the endothelial cells. Scale bar=50  $\mu\text{m}$ . Green auto-fluorescent was noted in outer segment (OS) and inner segment (IS) layers. Open arrow: TUNEL positive retinal EC cell; solid arrow: non-EC TUNEL positive cell in the retina.

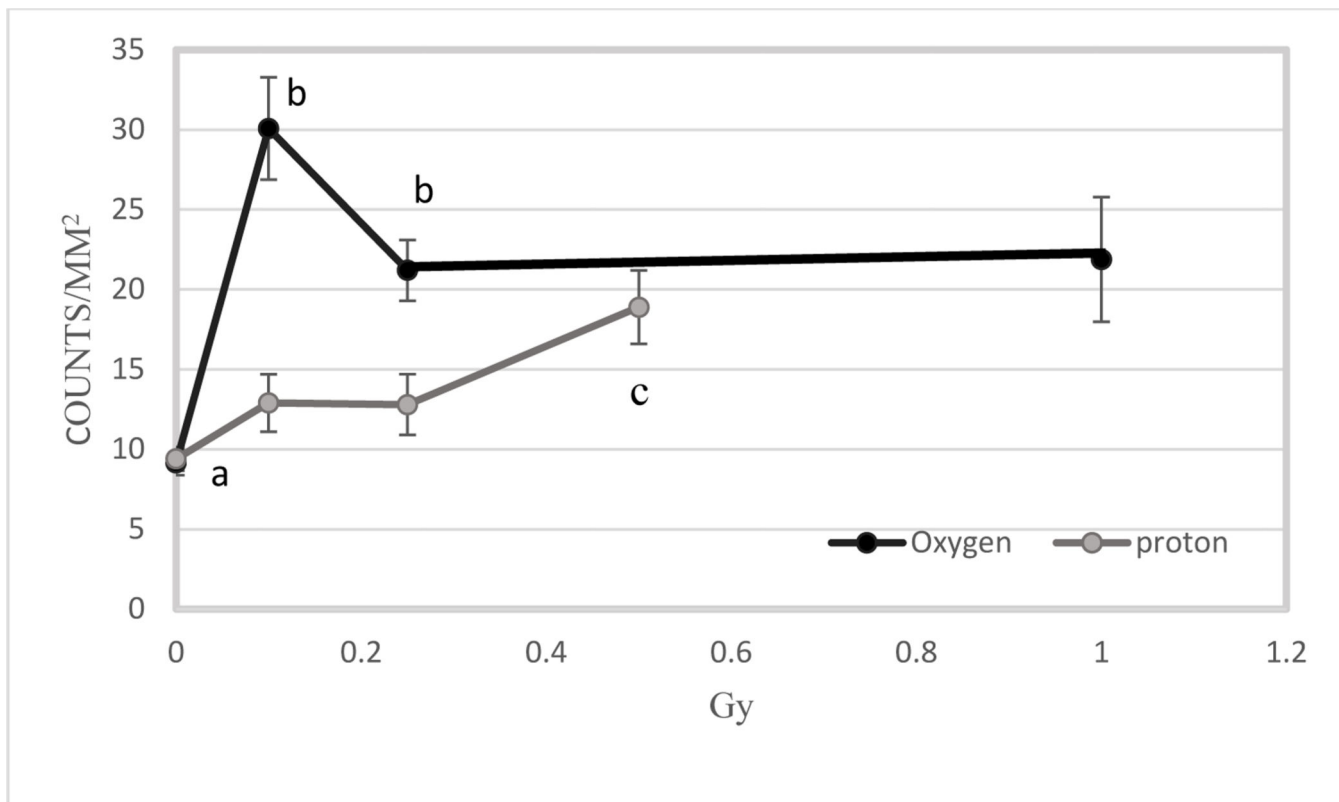


**Figure 2:** Comparison of radiation-induced apoptosis in retinal endothelium between  $^{16}\text{O}$  ions and protons at the 2-week time point. Quantification of TUNEL immunoreactivity is based on density profile of TUNEL-positive endothelial cells in the retina 2 weeks after  $^{16}\text{O}$  or proton exposure. Values are represented as mean density  $\pm$  SEM for 8–10 mice/group. <sup>a</sup> significantly lower than all other  $^{16}\text{O}$  groups ( $p < 0.05$ ) <sup>b</sup> significantly higher than their counterparts ( $p < 0.05$ ). <sup>c</sup> significantly higher than other proton groups ( $p < 0.05$ ).

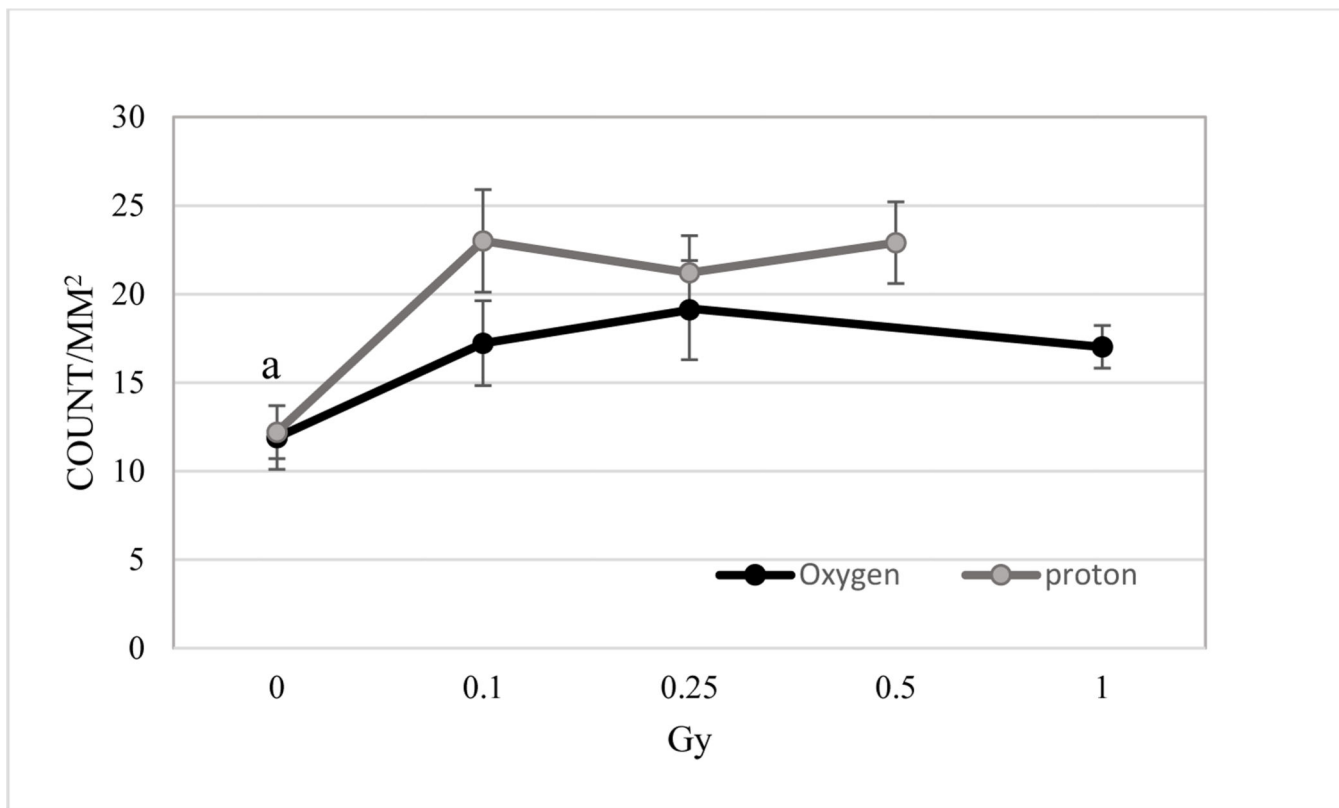


**Figure 3:** Immunoreactivity of TUNEL staining in the non-endothelium retinal cells. Quantification of TUNEL immunoreactivity is based on density profile of total TUNEL-positive cells minus the positive for endothelial cells in the retina at 2 weeks after  $^{16}\text{O}$  or proton exposure. Values are represented as mean density  $\pm$  SEM for 8–10 mice/group. <sup>a</sup> significantly lower than all other irradiated groups ( $p < 0.05$ ).

## ENOS, Endothelium, DAPI

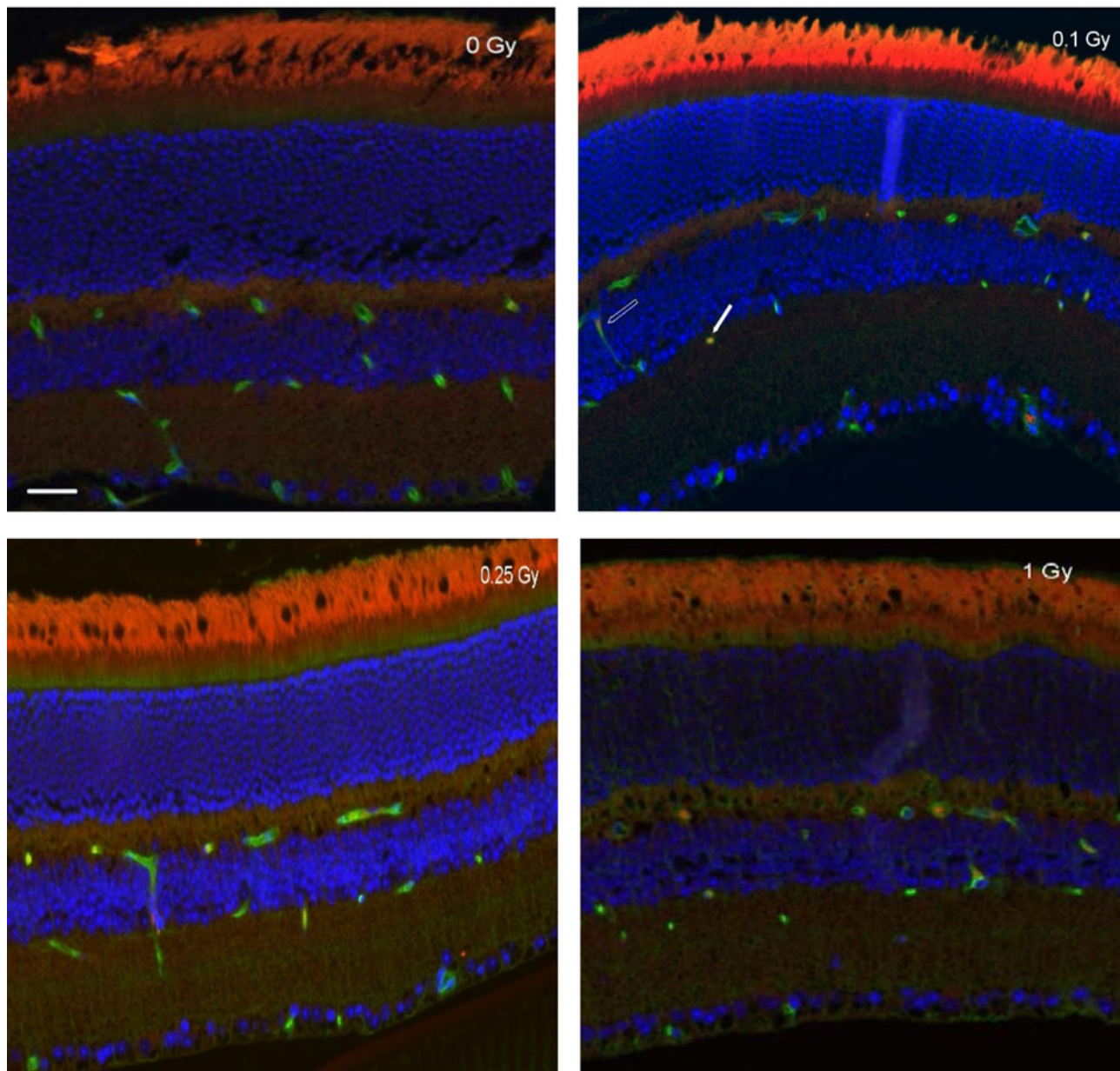


**Figure 4:** eNOS immunoreactivity in the retina following  $^{16}\text{O}$  irradiation. Representative micrographs of retina sections were evaluated at 2 weeks after  $^{16}\text{O}$  radiation. a) sham irradiated control, b) 0.1 Gy, c) 0.25 Gy and d) 1 Gy. eNOS positive cells were identified with red fluorescence, endothelium was stained with lectin (green). The nuclei of photoreceptors were counterstained with DAPI (blue). In the non-irradiated retinal tissue, only sparse eNOS-positive cells were found. In the retina from mice exposed to 0.1–1 Gy of  $^{16}\text{O}$  radiation, eNOS-positive labeling was apparent in the endothelial cells. Scale bar = 50  $\mu\text{m}$ . Red auto-

fluorescent was noted in outer layers. Open arrow: eNOS positive EC cell; solid arrow: non-EC eNOS positive cell in the retina.

Author Manuscript

Author Manuscript

Author Manuscript

Author Manuscript

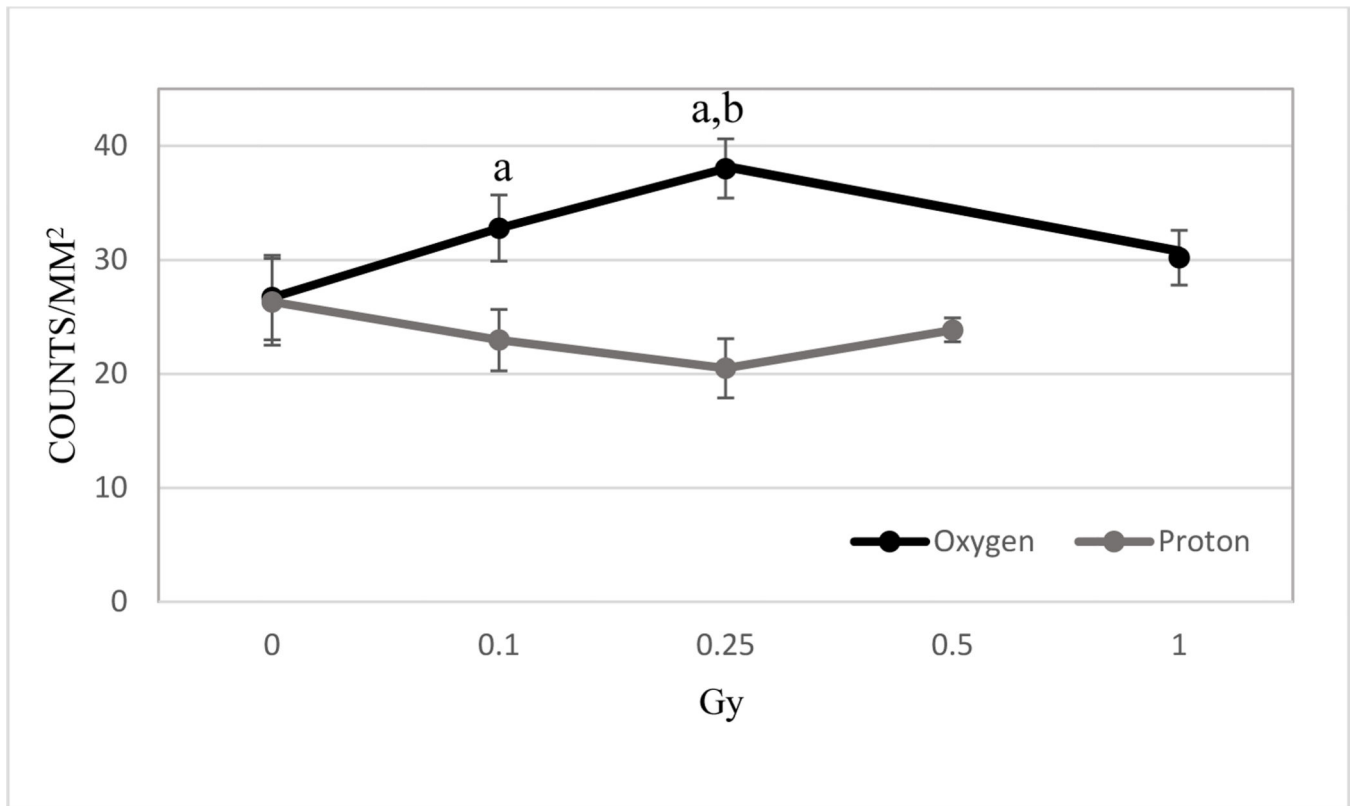


**Figure 5:** Comparison of radiation-induced eNOS expression in retinal endothelial cells between <sup>16</sup>O ions and protons at the 2-week time point. Quantification of eNOS immunoreactivity is based on density profile of eNOS-positive cells in the retinal endothelial cells at 14 days after <sup>16</sup>O or proton exposure. Values are represented as mean density  $\pm$  SEM for 8–10 mice/group. <sup>a</sup> significant higher proton counterparts ( $p < 0.05$ ) <sup>b</sup> significant higher than control group ( $p < 0.05$ ).



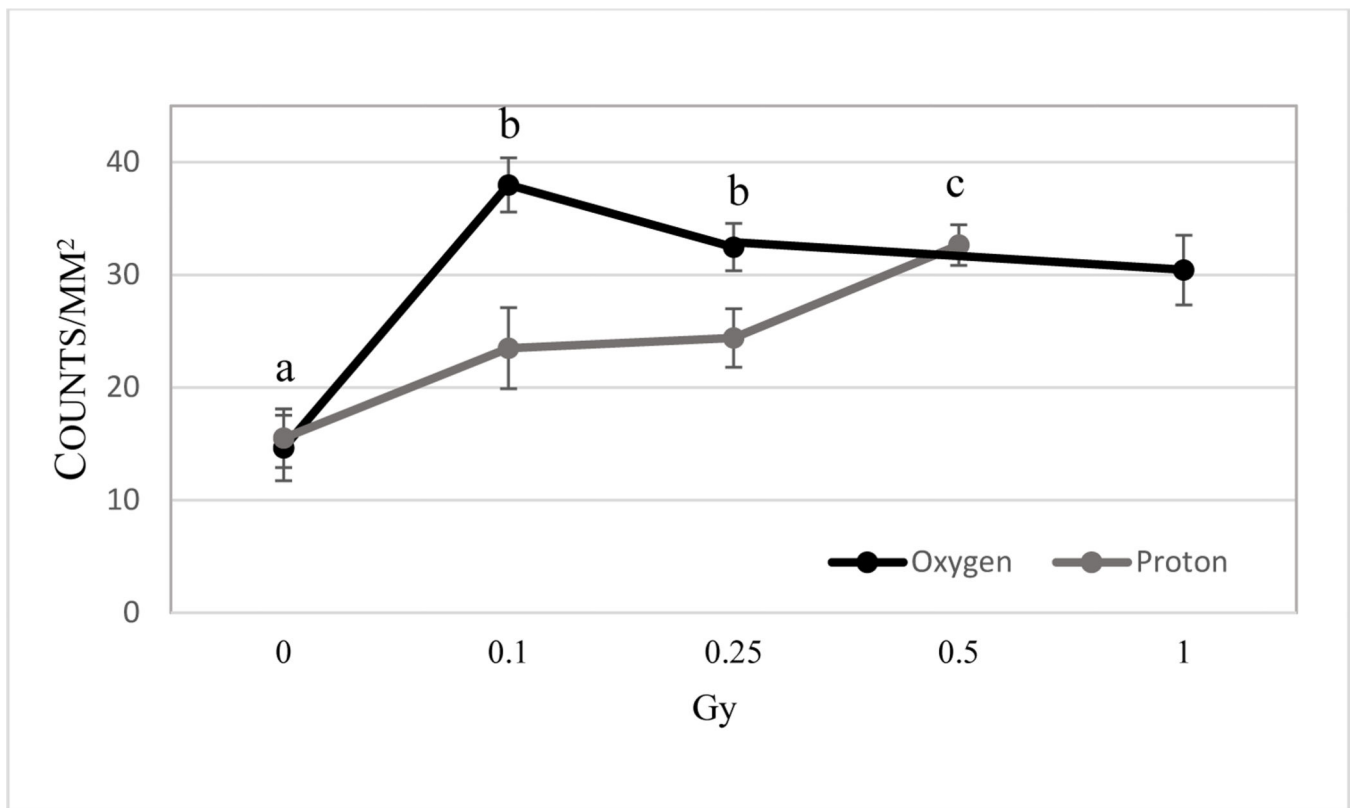


**Figure 6:** Comparison of radiation-induced eNOS expression in non-endothelium related retinal cells between  $^{16}\text{O}$  ions and protons at the 2-week time point. Values are represented as mean density  $\pm$  SEM for 8–10 mice/group. <sup>a</sup> significantly lower than all other  $^{16}\text{O}$  irradiated groups ( $p < 0.05$ ). <sup>b</sup> significantly higher than proton counterparts ( $p < 0.05$ ). <sup>c</sup> significantly higher than control and 0.25 Gy proton groups ( $p < 0.05$ ).

**Table 1:**

Determination of RBEM values for total number of apoptotic cells in the retina. RBEM values were based on fitting data to 2nd order polynomials and determining the slopes of the first derivative at  $D = 0$ .

Radiation	2 <sup>nd</sup> Order Polynomial Fit	R <sup>2</sup>	1 <sup>st</sup> Derivative	Slope at D = 0	RBE <sub>M</sub>
Gamma	$y = -3.26D^2 + 43.0D + 25.8$	0.91	$y = -6.52D + 43.0$	43.0	1.00
Protons	$y = -63.2D^2 + 68.8D + 24.0$	0.80	$y = -126D + 68.0$	68.8	1.60
Oxygen	$y = -88.7D^2 + 97.9D + 23.0$	0.84	$y = -177D + 97.9$	97.9	2.28